SLAC-PUB-1881
February 1977
(T/E)

RELATIVISTIC INTERACTIONS BETWEEN NUCLEI*

I. A. Schmidt† and R. Blankenbecler

Stanford Linear Accelerator Center
Stanford University, Stanford, California 94305

ABSTRACT

A relativistic theory of the inclusive scattering of nuclei is given. The theory is applicable to meson production reactions as well as to the yields of light nuclei. A characterization of the relativistic nuclear wave function is given and its connection to the standard wave function is explicitly shown. Counting rules are derived that allow one to simply characterize the behavior of the reaction cross sections in terms of the short range behavior of the nucleon-nucleon force. Good agreement with experiment is achieved if the force is assumed to be due to the exchange of vector mesons with monopole form factors at each vertex. The predictions are successfully compared to several reactions.

(Submitted to Phys. Rev. D.)

---

*Work supported by the Energy Research and Development Administration.

†On leave from: Universidad Técnica Federico Santa María, Valparaíso, Chile.

I. INTRODUCTION

Recent experiments[1-5] using very high energy heavy ion beams have created considerable theoretical interest.[6-10] A relativistic, yet simple, theory for these reactions would be extremely useful. In this paper we shall develop a convenient theory for this type of reaction, make predictions based on various models of the nucleon-nucleon force, and compare with the experimental data.

Our discussion will be based on a generalization of the relativistic hard-collision models of composite hadrons.[11] In the application of this picture to interactions of nuclei, the constituents ("partons") are nucleons, whose characteristics are well known. One suspects that this type of model must work with sufficiently general wave functions and interactions, and the main question is one of relative simplicity. In a restricted sense, this application can serve as a test case for the ideas and interpretations presently used in the hadron-quark models of strong interactions. However, in its own right, it can be used to extend the theory of the scattering of composite systems to the relativistic domain, and to extract important properties of the nuclear force.

We shall for the most part concentrate on the kinematic regime that explores the short distance behavor of the nuclear wave functions. This is only a small fraction of the total reaction cross section, but perhaps it is the most interesting part because it is unexplored. One can easily extend the range of applicability of our predictions by making a more complicated ansatz for the nuclear wave functions to match on to the nonrelativistic regime, where it is best known, but this will not be done here. This extension deserves further study.

The effects of shadowing and rescattering will also be neglected in our treatment. Hence the treatment given here should be most applicable to light nuclei. A careful study of this phenomenon in the present case could be very

interesting in trying to understand the anomalous nuclear effects observed in large transverse momentum events.[12]

The recent availability of excellent data on heavy ion reactions at high energies,[1-5] which necessitates a relativistic description of the process, motivated the present investigation. We hope to show that this type of data explores new aspects of the nuclear wave function which have a very simple interpretation in terms of the basic interactions between nucleons in the nucleus. The large q^2 behavior of the nuclear electromagnetic form factor explores a similar regime.[13]

This paper is organized as follows. In Section II the model is presented, using convenient parametrizations for the momenta and defining the distribution functions of nucleons in the nucleus $G(x,\vec{k}_T)$. As we will see, these distribution functions are explicitly measured in the experiments we are considering. Section III discusses in detail the nonrelativistic limit of these functions, which gives us useful information about their behavior and parametrization. In order to incorporate characteristics that are essentially relativistic, we develop in Section IV convenient "counting rules" for different theories of the nucleon-nucleon interaction that can be used to characterize our predictions. We then get a form for G that has the correct nonrelativistic limit, and at the same time expresses in a simple way the basic short range interaction between the constituents. In order to have simple predictions that can easily be compared with experiments, a high energy approximation is developed in Section V. We get in this limit, several results that are stated in Sections VI and VII for π^- and p production. A more accurate kinematic treatment is given and the above simple results are shown to have a rather wide validity. Quasi-elastic scattering is also discussed in some detail. Explicit comparison with experiment is made for

several cases. A discussion of the results is presented in Section VIII, emphasizing the generality and simplicity of our approach.

II. HARD SCATTERING MODEL

In a general inclusive reaction involving nuclei, the detected particles with momenta (either longitudinal or transverse) substantially different from the initial beam or target are assumed to arise from a direct internal interaction of constituents. These constituents may be nucleons or composite states that are virtually present in the nucleus, such as deuterons, alpha particles, etc. The fundamental diagram to be considered here for the process $A+B \rightarrow C+X$ is given in Fig. 1. Shadowing and rescattering have obviously been neglected. Here M_0 is the amplitude for the basic process $a+b \rightarrow C+d$, where the incident states a and b are off-shell. The simplest type of basic process is quasi-elastic scattering, $n+n \rightarrow n+n$, where n means either a proton or neutron (we shall not differentiate between them in our notation or treatment), and perhaps the next simplest is $n+n \rightarrow \pi+X$.

Our procedure will be to take M_0 from experiment, where it is given only on-shell, and to make an extrapolation according to a prescription to be given later (this extrapolation has very little effect on our predictions). Another more fundamental way to proceed would be to go one step further and predict M_0 in terms of the interactions of the constituents of the hadrons. This will not be done because it is a more difficult task. However, it is interesting to point out that all our fitted behavior of the various M_0's are consistent with the behavior expected in constituent models. Finally, the effects of spin will be neglected here. Its inclusion would allow interesting polarization effects and the spin structure of the short range nuclear force to be studied.

For the analysis of the diagram of Fig. 1, it is convenient to parametrize the different momenta using "infinite momentum frame" variables as follows:

$$A = \left(P_1 + \frac{A^2}{4P_1},\ \vec{0}_T,\ P_1 - \frac{A^2}{4P_1}\right)$$
$$B = \left(P_2 + \frac{B^2}{4P_2},\ \vec{0}_T,\ -P_2 + \frac{B^2}{4P_2}\right) \qquad (1)$$

where a particle's name and four-momentum are denoted by the same symbol except for the off-shell particles a and b. A and B have been defined in a general set of frames along the interaction axis. A specific frame in this set is selected by relating P_1 and P_2. For example, the center-of-mass frame is defined by the conditions

$$P_1 - \frac{A^2}{4P_1} = P_2 - \frac{B^2}{4P_2}$$

and

$$\sqrt{s} = P_1 + \frac{A^2}{4P_1} + P_2 + \frac{B^2}{4P_2} \quad .$$

This rather cumbersome set of variables will greatly simplify our later discussion. Also we define the other momenta that are on-shell as

$$\alpha = \left((1-x)P_1 + \frac{\alpha^2+k_T^2}{4(1-x)P_1},\ -\vec{k}_T,\ \ (1-x)P_1 - \frac{\alpha^2+k_T^2}{4(1-x)P_1}\right)$$
$$\beta = \left((1-y)P_2 + \frac{\beta^2+\ell_T^2}{4(1-y)P_2},\ -\vec{\ell}_T,\ -(1-y)P_2 + \frac{\beta^2+\ell_T^2}{4(1-y)P_2}\right) \qquad (2)$$

Note that with these parametrizations, the phase space integrals are of the form

$$d^4\alpha = d^2k_T \frac{dx}{2|1-x|} d\alpha^2 \qquad (3)$$

The off-shell momenta are calculated by momentum conservation:

$$a = \left(xP_1 + \frac{k^2+k_T^2}{4xP_1}, \vec{k}_T, xP_1 - \frac{k^2+k_T^2}{4xP_1} \right)$$
$$b = \left(yP_2 + \frac{\ell^2+\ell_T^2}{4yP_2}, \vec{\ell}_T, -yP_2 + \frac{\ell^2+\ell_T^2}{4yP_2} \right) , \tag{4}$$

where

$$k^2 = \left(x(1-x)A^2 - x\alpha^2 - k_T^2 \right)/(1-x)$$
$$\ell^2 = \left(y(1-y)B^2 - y\beta^2 - \ell_T^2 \right)/(1-y) \quad . \tag{5}$$

Note that with these parametrizations,

$$x = \frac{a_0+a_3}{A_0+A_3}$$

which is the usual light-cone variable.

Using the Feynman rules, it is a simple matter to evaluate the diagram of Fig. 1. After squaring and integrating over the final state phase space of d and α and β (which can have a mass spectrum and does not need to be a definite state—this only generalizes the definition of the G function defined below), the inclusive cross section

$$E_C \frac{d\sigma}{d^3C} \equiv R_C$$

achieves the form

$$R_C = \sum_{a,b} \int dx\, d^2k_T\, dy\, d^2\ell_T\, G_{a/A}(x, \vec{k}_T)\, G_{b/B}(y, \vec{\ell}_T)$$
$$r(s', s, x, y) \left[E_C \frac{d\sigma}{d^3C} (a+b \to C+d; s', t', u') \right]$$

where

$$r = \frac{\lambda(s', k^2, \ell^2)}{xy\,\lambda(s, A^2, B^2)}$$

and where the x and y integrals run only from zero to one. The variables s', t', u' are those that describe the internal basic process and defined in terms of a, b, and C. The G functions will be defined below. The ratio r of the λ factors is the ratio of the corresponding phase space factors in the cross sections, and

$$\lambda^2[x, y, z] \equiv x^2 + y^2 + z^2 - 2(xy+yz+zx) \quad .$$

One finds that throughout the range of variables we are interested in, $r \approx 1$.

A precise definition of the variables will be made later, but the interpretation of the various factors in Eq. (6) is clear. The factor $G_{a/A}(x, k_T)$ is the probability of finding a constituent of type a in nucleus A with fractional "momentum" x and transverse momenta k_T. A similar interpretation holds for $G_{b/B}$. The basic cross section factor that actually produces the detected particle C also has a clear probabilistic meaning.

The probability functions are defined as

$$G_{a/A}(x, \vec{k}_T) = \frac{1}{2(2\pi)^3} \frac{x}{(1-x)} |\psi(x, \vec{k}_T)|^2 \qquad (7)$$

where ψ is the bound state Bethe-Salpeter wave function with one leg (α) on-shell. It is related to the vertex function ϕ by

$$\psi(x, \vec{k}_T) = \frac{\phi}{k^2 - a^2} \quad . \qquad (8)$$

One can also derive an equation for the electromagnetic form factor of the state A in terms of ψ and the result is

$$F_A\left(q_T^2\right) = \frac{1}{2(2\pi)^3} \int \frac{x\,dx}{(1-x)}\, d^2k_T\, \psi^*(x, \vec{k}_T)\, \psi\left(x, \vec{k}_T - (1-x)\,\vec{q}_T\right) \qquad (9)$$

Let us now turn to a more detailed discussion of the probability functions and their interpretation.

III. THE NONRELATIVISTIC LIMIT

In order to have a clear understanding of the G functions, and how they are expected to behave, it is instructive to make a nonrelativistic approximation. This should also allow us to explore the way in which masses enter into the analysis. The G function must be very closely related to the square of the nonrelativistic wave function but the peculiar variables x and k_T do not seem to be closely related to the familiar $\vec{k}$ of Schrœdinger theory. Their interpretation is quite simple, however.

Consider the factor of (k^2-a^2) that occurs in ψ and define

$$M^2(x) \equiv (1-x)(a^2-k^2) - k_T^2$$

$$= (1-x)a^2 + x\alpha^2 - x(1-x)A^2 \quad . \tag{10}$$

This function minimizes at $x=x_0$, where

$$x_0 = \frac{A^2+a^2-\alpha^2}{2A^2} \tag{11}$$

and this suggests writing

$$x = x_0 + \frac{k_z}{A} \quad .$$

One then finds

$$(1-x)(a^2-k^2) \cong a\epsilon + \vec{k}^2 \quad , \tag{12}$$

where it has been assumed that the binding energy per nucleon ϵ of the states A and α are the same. In this case one finds $x_0 \sim a/A$, i.e., each nucleon carries the same fraction of the total momentum of the nucleus at the peak of the wave function.

function. The G function becomes in this limit of small k_z:

$$G \equiv |\psi_{NR}(\vec{k})|^2 \sim \frac{\phi^2_{NR}(\vec{k})}{\left[a\epsilon+\vec{k}^2\right]^2}$$

where

$$\phi^2_{NR} \sim x_0(1-x_0)\phi^2 \quad .$$

The Schrœdinger equation in momentum space is of the form

$$\psi_{NR}(\vec{k}) = (a\epsilon+\vec{k}^2)^{-1} \int d^3p\, V(\vec{k}-\vec{p})\, \psi_{NR}(\vec{p})$$

$$\equiv (a\epsilon+\vec{k}^2)^{-1}\, \phi_{NR}(\vec{k}) \quad ,$$

so that the vertex function ϕ_{NR} expresses more or less directly the behavior of the potential V. The falloff of ϕ is related to the softness (or hardness) of the potential. As a simple example, consider a general Hulthen model of the nuclear wave function:

$$\psi_{NR} = (a\epsilon+\vec{k}^2)^{-1} \left(a\epsilon_1+\vec{k}^2\right)^{\frac{1-g}{2}} \quad .$$

A relativistic version of this wave function can be achieved by writing

$$\psi = \frac{N(x)}{(k^2-a^2)} \frac{1}{\left(k_1^2-a_1^2\right)^{\frac{g-1}{2}}} \quad , \tag{13}$$

where N(x) is slowly varying for x near 1 and defining

$$M_1^2(x) = (1-x)\left(a_1^2-k_1^2\right)-k_T^2$$

$$\equiv (1-x)a_1^2+x\alpha_1^2-x(1-x)A^2 \quad , \tag{14}$$

with $a_1^2 \equiv a^2+\delta^2$, $\alpha_1^2 \equiv \alpha^2+\delta^2$. Proceeding as before, one finds for small k_T and k_z:

$$G \cong C(x_0) \left[a\epsilon+\vec{k}^2\right]^{-2} \left[a\epsilon_1+\vec{k}^2\right]^{1-g} \tag{15}$$

where

$$C(x) = x(1-x)^g N^2(x) \quad , \tag{16}$$

$$M_1^2(x) = M^2(x) + \delta^2 \quad ,$$

and

$$a\epsilon_1 \equiv a\epsilon + \delta^2 \quad .$$

For the familiar Hulthen deuteron case, one usually chooses g=3 and $\epsilon_1 \sim 36\epsilon$. Thus $\delta^2 \sim 35a\epsilon$, and the second factor is much flatter in $\vec{k}^2$ than the first.

The form factor for this type of wave function is easily seen to fall as

$$F^2\left(q_T^2\right) \sim \left(q_T^2\right)^{-g-1}$$

for large q_T^2. Thus the falloff of the form factor and the behavior of G for large k_T^2 are closely related and also we see that the behavior of G for $x \sim 1$ is also closely related to the form factor falloff. This latter relation is the Drell-Yan-West relation.[14]

For general x, the relativistic G function can then be written as

$$G(x, \vec{k}_T) = N^2(x)\, x(1-x)^g \left[M^2(x) + k_T^2\right]^{-2} \left[M_1^2(x) + k_T^2\right]^{1-g} \quad . \tag{17}$$

For $x \sim x_0$, the denominator factors are rapidly varying and as has been discussed, this reduces to a familiar nonrelativistic Hulthen form. For $x >> x_0$, the numerator factors control the behavior of G, and

$$G(x, \vec{k}_T) \sim (1-x)^g$$

while its large k_T^2 behavior is $\left(k_T^2\right)^{-g-1}$.

In this paper, the behavior of G for $x >> x_0$ will be especially important. Note that this is new information not directly contained in the nonrelativistic wave function. We shall also discuss quasi-elastic scattering which explores the G function for $x \sim x_0$ as well. Let us now turn to a discussion of the calculation of the power g in selected theories of the nucleon-nucleon interaction.

IV. COUNTING RULES

In this section, the choice of appropriate wave functions will be discussed. This is not a trivial matter since one would like to have wave functions that reduce to familiar forms in the nonrelativistic limit but yet reflect the correct relativistic behavior (for large k_T and for $x \sim 1$) arising from a specific theory of the nucleon-nucleon interaction. Once the wave function is given, our main contact with experimental data is through the structure functions $G(x, k_T)$. A helpful tool for expressing the predictions of specific theories is in terms of "counting rules". These allow one to characterize the asymptotic behavior of G in terms of the number of constituents and the basic interactions of the theory.

The procedure here is to extract the leading behavior from the lowest order diagram in perturbation theory. For "soft" theories, one can show that the higher orders either are small compared to the leading term or have the same behavior. Consider the wave function (or structure function) diagram given in Fig. 2, where k is the momentum of particle a and is defined by Eq. (4). We shall assume scalar particles for simplicity. Note that A now also means the atomic number of particle A.

A

For a renormalizable interaction between the constituents, such as $\lambda\phi^4$, (vector exchange also is in this category) the falloff of the vertex function arises solely from the constituent propagators. One finds

$$\phi \sim \left(k_1^2 - a_1^2\right)^{1-n} \quad ,$$

where the masses in k_1 (see Eq. (14)) depend on detailed properties of the force. The wave function is

$$\psi \sim \left(k^2 - a^2\right)^{-1} \left(k_1^2 - a_1^2\right)^{1-n} \quad . \tag{18}$$

Comparison with Eq. (13) immediately tells us that

$$g = 2A - 3 \tag{19}$$

This is the usual dimensional counting prediction for the structure function[15] where one counts nucleons (assumed to be structureless point particles).

B

For a superrenormalizable theory, such as $\phi^2\chi$ (scalar exchange), the vertex function behaves as

$$\phi \sim \left(k_1^2 - a_1^2\right)^{1-n} \left(k_2^2 - a_2^2\right)^{-n} \quad , \tag{20}$$

where the additional factor arises from the falloff of the gluon propagators. The masses in k_2^2 are to be chosen appropriately. The prediction for g is

$$g = 4A - 5 \quad , \tag{21}$$

which reflects the increased softness of the potential.

C

As a final and perhaps most relevant example, consider a nucleon-nucleon interaction mediated by the exchange of vector mesons, such as rhos or omegas, with a monopole form factor at each vertex (vector dominance would assume such a behavior to fit the dipole nucleon form factor). One finds

$$\phi \sim \left(k_1^2 - a_1^2\right)^{1-n} \left(k_2^2 - a_2^2\right)^{-2n} \tag{22}$$

where the masses in the form factors and/or gluon propagators are chosen to be the same for simplicity. The final result is

$$g = 6A - 7 \quad . \tag{23}$$

This is the same result as found in a $\lambda\phi^4$ theory with a dipole form factor at each four-point vertex, and also is exactly the same result one would get by counting quarks. While one might expect that the quark degrees of freedom become relevant at ultra high energies where they can be excited, we see that one gets the same prediction for g in this theory when the nucleon form factor effects

play a role. These, of course, may in turn be due to internal structure, but these internal degrees of freedom need not be fully excited.

D

For more general structure functions $G_{a/A}$, where the state a is a bound state of a nucleons, a similar analysis can be carried through. One finds in this case

$$g = 2T(A-a) - 1 \tag{24}$$

where T=1, 2, or 3 depending upon the theory as discussed earlier.

E

Now that it is clear that one can differentiate between theories of the nucleon force by extracting values of g from the data, let us turn to a more detailed discussion of the probability functions.[16] The G's that will be considered here are all of the form (see Eq. (17))

$$G_{a/A}(x, \vec{k}_T) = \frac{N^2(x)\, x(1-x)^g}{\left[k_T^2 + M^2(x)\right]^2 \left[k_T^2 + M_1^2(x)\right]^{g-1}} \tag{25}$$

where N(x) is a slowly varying function of x, and

$$M^2(x) = (1-x)a^2 + x\alpha^2 - x(1-x)A^2$$

$$M_1^2(x) = M^2(x) + \delta^2 \quad .$$

For large values of A, g is large, and the second term in the denominator controls the falloff in k_T^2. For small k_T^2, G becomes

$$G \propto e^{-R^2 k_T^2}$$

where

$$R^2 \cong \frac{2}{M^2(x)} + \frac{g-1}{M_1^2(x)}$$

For $x \sim x_0$, one expects $R \sim A^{1/3}$, the normal nucleon radius, and hence $M_1^2(x_0) \sim A^{1/3}$. This is then a restriction on the behavior of the parameter δ^2 introduced before. In any case one can fit it directly from the above relation.

The general form for G that we have adopted, Eq. (24), has several properties that are worth noting:

- G is peaked at $k_T=0$ and the transverse momentum distribution falls more and more rapidly as A increases.
- G is peaked at $x \sim a/A$. The most likely momentum configuration is that one in which the nucleons share equally the total momentum of the nucleus.
- The power g which controls both $x \sim 1$ and large k_T is very simple to characterize in terms of the basic binding interaction and the number of constituents.
- The shape of G in the nonrelativistic limit does not restrict the behavior for $x \sim 1$ for general models (although they are strongly correlated in our simple models). A measurement of G for $x \sim 1$ is new information that is not accessible to conventional nuclear theory.

V. HIGH ENERGY LIMIT

In order to get simple predictions that can easily be compared with experiment without extensive numerical calculation, we will first analyze the situation in which the energy per nucleon is large compared to the nucleon mass. The kinematics for this regime is quite simple:

$$\begin{aligned} s' &= xys \\ t' &= yt \\ u' &= xu \\ d^2 &= xys + yt + xu \end{aligned} \tag{26}$$

and

$$C_T^2 = \frac{ut}{s}$$

The condition $d^2 > 0$ restricts the range of x and y that contribute for fixed values of s, t, u.

Projectile fragmentation region. When t is fixed (and s, u large), one finds

$$1-x_F = 1 + \frac{t+u}{s}$$

and

$$1-x'_F = 1 + \frac{yt+xu}{xys} \tag{27}$$

and hence $x'_F \cong x_F/y$. The condition $d^2 > 0$ becomes $y > x_F$. In this regime formula (6) becomes

$$R_C \sim \sum_{ab} \int_0^1 dx\, d^2k_T\, G_{a/A}(x, \vec{k}_T) \int_{x_F}^1 dy\, d^2\ell_T\, G_{b/B}(y, \vec{\ell}_T) \left[E_C \frac{d\sigma}{d^3C}\right]^1 . \tag{28}$$

All inclusive basic processes of interest to us here will be parametrized as

$$\left[E_C \frac{d\sigma}{d^3C}\right]^1 = E(s') \left(1 - |x_F|\right)^H e^{-r^2 k'^2_T} \tag{29}$$

and exclusive processes as

$$\left[E_C \frac{d\sigma}{d^3C}\right]^1 = E(s')\, \delta\left[(k+\ell-C)^2 - d^2\right] e^{-r^2 k'^2_T} \tag{30}$$

where $k'_T = C_T - k_T - \ell_T$ and E(s') is assumed rather slowly varying. H will be assumed to be constant, but a dependence on transverse momentum can easily be included.

Since the exponentials are strongly peaked in k'^2_T, we can approximate the k_T and ℓ_T integrals by replacing k_T^2 and ℓ_T^2 in the G's by the mean value K^2 which should be of the order of C_T^2. The inclusive cross section is then proportional

to

$$R \propto \int_{x_F}^{1} dy \frac{N^2(y)\, y(1-y)^{g_B}}{\left[K^2+M^2(y)\right]^2 \left[K^2+M_1^2(y)\right]^{g-1}} \left(1 - x_F/y\right)^H \quad . \tag{31}$$

Note that the distribution for the target $G_{a/A}$ has integrated out in this limit, and that R depends on A through its normalization only.

If $C_T^2 \gtrsim M_1^2(x_0)$, and if x_F is not small compared to x_0, then the main variation in the integrand is from the factors of (1-y) and $(1-x_F/y)$. The first factor cuts off the integrand near y=1 and the other near $y=x_F$. If only their variation is retained, and the denominators taken constant, we have

$$R \propto \int_{x_F}^{1} dy (1-y)^{g_B} \left(1 - x_F/y\right)^H$$

$$R \sim \left(1 - x_F\right)^{g_B+H+1} \quad . \tag{32}$$

A more accurate treatment is possible but the above will suffice for our purposes. In the target fragmentation region, where u is fixed and s, t large, the above arguments can be repeated with the result that

$$R \sim \left(1 + x_F\right)^{g_A+H+1} \quad , \tag{33}$$

where g_A is the power behavior of the target distribution function $G_{a/A}$. This result could also have been achieved by simply interchanging the target and beam particles in the previous result. These predictions will be compared to data in a later section.

One can estimate the range of validity in x_F of the above formulas by a simple argument. The momentum fraction x_F must be large enough so that the particle is out of the "quasi-elastic" peak where the denominator factors in Eq. (31) are rapidly varying. The average momentum fraction x_B of particle B

is $\langle x_B \rangle = 1/B$. The average x retained by the detected particle of Eq. (29) is roughly $\simeq 1/(H+2)$. Therefore, the behavior given by Eq. (32) should hold reasonably well for $x_F \gtrsim 1/B(H+2)$. For example, for the process deuterons $\rightarrow \pi^-$, this limit is $x_F \gtrsim 1/2\times 5 = 1/10$, and most of the x_F range is covered.

For an exclusive basic process, which yields a familiar quasi-elastic reaction, the calculation is also quite simple. Using Eq. (30) and expanding the arguments of the delta function for the case $b+n \rightarrow C+n$, where b and C are nucleons, one finds that a reasonable approximation is:

$$\left[E\frac{d\sigma}{d^3C}\right]^1 = E(s')\,\delta\left[x(s-A^2-B^2)(x_F-\Delta-y)\right]\, e^{-R^2k_T'^2}$$

where the shift Δ has to be calculated using more exact kinematics. At high energies $\Delta \rightarrow 0$.

Again the x integral is not restricted and the full inclusive cross section is

$$R \propto G_{C/B}\left(x_F-\Delta, K^2\right)\left(\frac{d\sigma}{dt}\right)^1 \qquad (34)$$

the quasi-elastic peak should occur at $x_F = C/B + \Delta$. This is slightly larger than the naive expectation C/B, the most likely momentum in the state B. This shift will be included in all our numerical calculations. Equation (34) can be interpreted as a relativistic generalization of the Glauber approximation but with a more precise definition of the covariant wave function.

Although for simplicity we have discussed in detail the kinematics of the high energy region only, it can be shown that our results should be quite accurate at lower energies. For example, one important conclusion of our analysis was that the lower limit of the y-integral is equal to x_F. This comes from the condition $(k+\ell-C)^2 > d^2$. We have calculated this equation more exactly, assuming small transverse momenta and $\langle x \rangle = d/A$, and found that the corrections are

small for the range of energies of the experiments we want to analyze here (kinetic energies per nucleon $\approx$1 or 2 GeV). At the quasi-elastic peak, for example, we find

$$\begin{aligned} \Delta &= .07 \quad (dC \rightarrow pX) \\ \Delta &= .05 \quad (CC \rightarrow pX) \\ \Delta &= .075 \quad (CC \rightarrow HeX) \end{aligned} \tag{35}$$

and these shifts show clearly in the experimental data (see Figs. 7 and 8). The values were calculated assuming a specific internal process. For example, in the case CC $\rightarrow$ HeX, the internal process was Hep $\rightarrow$ HeX. Another possibility could have been He+He $\rightarrow$He+X, but this gives a shift at the quasi-elastic peak that does not agree with the experimental data. The position of the quasi-elastic peak is determined by the nature of the fragment b arising from the beam. The kinematical shift Δ then determines the fragment, a, arising from the target. Additional subsidiary peaks or shoulders in the data could be due to more than one basic process being important. These can be identified using the above procedure even if the dominant ones change with angle.

VI. PION PRODUCTION

As the first application of the model, we shall consider π^- production in several different reactions. The data in Fig. 3, taken from J. Papp et al.,[2] clearly supports a prediction of the model that the cross section does not depend upon the target except for an overall factor (which goes as $A^{1/3}$ due to the circumferential nature of the scattering) except very near threshold.

A proper treatment of these kinematic effects is necessary in certain kinematic regions. For example, one expects that in the fragmentation region of processes such as p+A $\rightarrow \pi^-$+X, the cross section will be the same as for p+p $\rightarrow \pi^-$+X. This is not so at the lower energies because of a kinematic

effect that is essentially the same for all targets ($A \geq 2$) and which changes the shape of the cross section. The point is that near threshold, the integration over x (the target longitudinal momentum variable) does not go from zero to one and actually the allowed interval shrinks to a point for $x_F \to 1$. Now k^2 is negative for most values of x, and for $x_F \sim 1$ some of the energy for the reaction must be extracted from the Fermi motion in the target.

The basic reaction $p+p \to \pi^- + X$ will be parametrized as

$$R' = R_0(1-x'_F)\, e^{-4x'_F}\, e^{-15k_T^2} \quad . \tag{36}$$

This is a reasonable representation to the data of Akerlof et al.[17] and E. Gellert.[18] We will treat neutrons and protons the same in order to keep the treatment simple.

$pC \to \pi^-$: Using the R' given above, and calculating numerically using exact kinematics, we get the result shown in Fig. 4. We have not computed the normalization (this would require a careful treatment of absorption) and have normalized our calculation to the data.[2] For energies in the range of interest, one finds that R scales (for different energies) and for fixed (small) t, that

$$R \propto (1-x_F)^3 \quad , \tag{37}$$

which is not very different from Eq. (36) except near $x_F=1$. Note that a change in the power by 1 is a factor of two difference at $x_F=0.6$ if normalized at $x_F=0.2$. This form does not depend upon the specific target distribution function and hence is the same for all the different counting rules. The properties of the target wave function do not enter except in the overall normalization constant.

For backward scattering, i.e., u-fixed, the result depends strongly on the theory of the target wave function. We find (A=12)

$$R \sim (1+x_F)^b$$

where b = 23, 45, 67 for the three possible theories (A, B, C, respectively) of the previous section.

DC $\rightarrow \pi^-$: From the analysis of the previous section, we know that H=3. The prediction for R should now depend upon the deuteron wave function. For t-fixed, we find

$$R \sim (1-x_F)^f \tag{38}$$

where f = 5, 7, and 9 for the three theories. If we compare with experiment,[2] Fig. 5, the value 9 is clearly favored. Recall that this is the theory of vector meson exchange (omegas or rhos) with monopole form factors. These counting rules are the same as quark counting, i.e., T=3.

For backward scattering, u-fixed, one finds

$$R \sim (1+x_F)^b$$

where b = 25, 47, 69 for the respective theories.

HeC $\rightarrow \pi^-$: This reaction clearly shows, see Fig. 6, the effects of strong correlation in the initial wave function since pions are observed with one-half of the incident alpha particle momentum. The predictions are

$$R \sim (1-x_F)^f \tag{39}$$

where f = 9, 15, and 21. The data[2] of Fig. 4 shows that f is definitely between 17 and 25, and 21 is a good fit. This data again favors model C, T=3.

In the backward direction, we find

$$R \sim (1+x_F)^b$$

where b = 25, 47, and 69.

We have also compared our predictions for forward scattering from beryllium and the agreement with the data of Ref. 4 is quite satisfactory.

VII. PROTON PRODUCTION

Now let us consider inclusive proton production. First, some examples will be discussed outside the quasi-elastic peak, that is, $x_F > 1/B$. Then quasi-elastic scattering will be treated. As we have stressed before, this is a test of the wave function in the relativistic regime, whereas the quasi-elastic peak depends upon the most likely nucleon configuration which can be adequately described by a nonrelativistic wave function.

As explained before, the effective internal cross section should include some kinematical effects arising from the target due to the low energy but this will be neglected here. From $pp \to pX$ data, we conclude that $H_{eff} \simeq -1$ (recall Eqs. (29) and (30)).

DC → P: For this case, the prediction follows just as in the pion case and one finds in the forward direction

$$R \sim (1-x_F)^f \tag{40}$$

where f = 1, 3, or 5 for the three theories. The data does not extend very far above the quasi-elastic peak. In Fig. 7 the prediction for f=5 is graphed. The data[3] seems to indicate that f is between 4 and 5. This is again consistent with theory C. The full curve in Fig. 7 will be discussed shortly.

For backward scattering, the prediction is

$$R \sim (1+x_F)^b$$

where b = 21, 43, and 65.

CC → P: Just to see how far our model can be pushed, consider this reaction. Obviously, the predicted powers are going to be very large but nevertheless

are susceptible to analysis. The consistency of this model can at least be tested and its trend as the nucleon number increases. In this case, the forward and backward predictions are the same and one finds

$$R \sim \left(1 - |x_F|\right)^f \tag{41}$$

where f=21, 43, or 65. The data from Ref. 3 in Fig. 8 seems to indicate a large value of f, with 65 being a quite acceptable fit, but more data is needed for a definitive test.

CC → He4: The predictions for f are 15, 31, or 47 if the intermediate state b is an alpha particle. In Fig. 8 the curve for f=47 is consistent with the data.[3] The other possibilities are nowhere near the experimental curve.

Quasi-elastic: We have computed quasi-elastic scattering for one sample process, DC → pX. The deuteron wave function was chosen from model C, so that g=5 and in order to get a reasonable rms radius, $\delta^2 = 200\, a\epsilon$. Setting $K^2 = \vec{C}_T^2$ in Eq. (34), one gets the curve shown in Fig. 7. The agreement is quite good throughout the peak region and above. The excess rate at low x_F must be due to multiple scattering in the nucleus which we have made no attempt to calculate.

We have compared predictions of the above type for beryllium target data[4] and the fit is satisfactory.

VIII. CONCLUSIONS

The model we have presented here is quite general and can be applied to many different types of reactions. Although in our presentation we have analyzed only the case of strong interactions, applications to deep inelastic electromagnetic and weak interactions in nuclei are also possible.

The effects of absorption were completely neglected in the present treatment, and this is a very important omission that must be remedied if one wishes to compute the absolute normalization of the reactions discussed here.

In conclusion, we feel that the general approach used here to describe the high energy scattering of heavy ions has many advantages over the conventional approach using Schrœdinger wave functions and standard scattering theory. Some aspects of our model that are worth mentioning are:

(1) We have presented a fully relativistic formulation of the scattering of bound states. The formalism has a very simple physical interpretation. The relativistic wave functions are shown to be simply related to familiar nonrelativistic choices. The relativistic situation is described in terms of distribution functions $G(x, \vec{k}_T)$, which can be explicitly measured, and which have a simple probabilistic interpretation.

(2) We have developed counting rules that allow one to predict in a simple way the general behavior of the reaction cross sections. These counting rules are expressed in terms of the basic short range behavior of the nucleon-nucleon force.

(3) Good agreement with several experiments is attained for one simple model. This model has as its basic force the exchange of vector mesons with monopole form factors at each vertex. The agreement with experiment holds for both meson production and proton inclusive processes. Once the force is given, there are no parameters (except for normalization) outside the quasi-elastic peak, and even this needs δ^2 only. It is important to add that we have checked several other reactions not included here, and all are consistent with the prediction of the counting rules for the same simple model.

(4) The force model that fits experiment is shown to have the same counting rules as the quark-dimensional counting model discussed by Brodsky and Chertok.[13] Since the reactions discussed here are certainly at too low an energy to fully excite the quark degrees of freedom, the agreement between the quark model and the elastic deuteron data can perhaps be more easily understood in terms of our model. Evidently, the theory is much smoother than one would expect a priori in its connection between very high energies (excitation of quark degrees of freedom) and the range of energies we have discussed here.

(5) Our results scale in the sense of being a function only of x_F, independent of the energy. This is clearly shown in the data. It is interesting to note that this is true even when all the effects of masses are included, as we checked explicitly by computing the cross section for the case ($p + C \rightarrow \pi^- + X$) numerically.

(6) The model used here provides a simple yet relativistic description of quasi-elastic scattering. It contains the standard Glauber theory and the standard impulse approximation in the low energy limit.

(7) Predictions are easily made and are given for as yet unmeasured processes which can serve as a more severe test of our model (backward scattering for example).

(8) The model allows one to simply describe a region of the wave function that cannot be described sensibly in the nonrelativistic approach. The experimental data is thus exploring a new regime of nuclear physics and providing new tests of nuclear theory.

Acknowledgments

We wish to thank S. J. Brodsky for several helpful conversations and H. Steiner for giving an excellent seminar that aroused our interest in this subject.

REFERENCES

1. For a review see B. Cork, in Proc. of the Int. Conf. on High Energy Physics and Nuclear Structure, Los Alamos, 1975, p. 598. Also H. Steiner, in High Energy Collisions Involving Nuclei, G. Bellini, L. Bertocchi, and P. G. Rancoita, eds. (Editrice Compositori, Bologna, 1975), p. 151.
2. J. Papp et al., Phys. Rev. Letters 34, 601 (1975).
3. J. Papp, Ph.D. Thesis, University of California, Berkeley, Report LBL-3633 (1975).
4. L. S. Schroeder, Report LBL-3362, presented at the Particles and Fields Meeting of the American Physical Society, Williamsburg (1974).
5. A. M. Baldin et al., Sov. J. Nucl. Phys. 18, 41 (1974).
6. G. F. Chew, Print-75-0222, University of California, Berkeley. This analysis is in terms of triple Regge theory. One can interpret our results as predictions of the values of "effective" Regge trajectories. See also F. Uchiyama, in Proc. High Energy Heavy Ion Summer Study, Lawrence Berkeley Laboratory, 1974, p. 293.
7. H. Feshbach and K. Huang, Phys. Lett. B 47, 300 (1973).
8. A. S. Goldhaber, "Statistical Models of Fragmentation Processes," presented at High Energy Heavy Ion Summer Study, Lawrence Berkeley Laboratory, 1974.
9. J. Lepore and R. Riddell, in Proc. High Energy Heavy Ion Summer Study, Lawrence Berkeley Laboratory, 1974.
10. L. Bertocchi and D. Treleani, CERN-TH-2203, preprint (1976).
11. R. Blankenbecler, S. J. Brodsky and J. F. Gunion, Phys. Rev. D 6, 2652 (1972). See also D. Sivers, S. J. Brodsky and R. Blankenbecler, Physics Reports C 23, No. 1 (1976).

12. J. W. Cronin et al., Phys. Rev. Letters 31, 1426 (1973). J. W. Cronin et al., Phys. Rev. D 11, 3105 (1975).

13. See S. J. Brodsky and B. T. Chertok, SLAC-PUB-1759, Stanford Linear Accelerator Center (1976), submitted to Phys. Rev. D.

14. S. D. Drell and T.-M. Yan, Ann. Phys. (N.Y.) 66, 578 (1971). G. West, Phys. Rev. Lett. 24, 1206 (1970).

15. R. Blankenbecler and S. J. Brodsky, Phys. Rev. D 10, 2973 (1974). For fixed angle counting rules see S. J. Brodsky and G. R. Farrar, Phys. Rev. Lett. 31, 1153 (1973); Phys. Rev. D 11, 1309 (1975).

16. We are generalizing and improving the hadron case treatment of C. Sachrajda and R. Blankenbecler (unpublished).

17. C. W. Akerlof et al., Phys. Rev. D 3, 645 (1971).

18. E. Gellent, LBL-784, preprint, Lawrence Berkeley Laboratory, presented at the Int. Conf. on Inclusive Reactions, Davis, California, 1972.

FIGURE CAPTIONS

1. The basic hard scattering model diagram with the notation used in the text.
2. The wave function diagram used to compute the probability functions.
3. Scattering from selected targets according to Ref. 2 to illustrate A independence of the shape of the x spectrum.
4. The x_F spectrum compared to the carbon data illustrating scaling.
5. The prediction for T=3 compared to the data of Ref. 2 for a deuteron beam.
6. The prediction for T=3 compared to the data of Ref. 2 for an alpha particle beam.
7. The prediction for inclusive protons from a deuteron beam for T=3. The full curve is a fit to the quasi-elastic peak using the theory in the text.
8. Two inclusive processes for a carbon beam illustrating the counting rules and the positions of the quasi-elastic peaks.

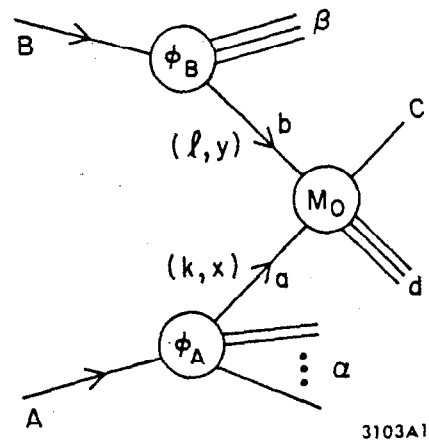

Fig. 1

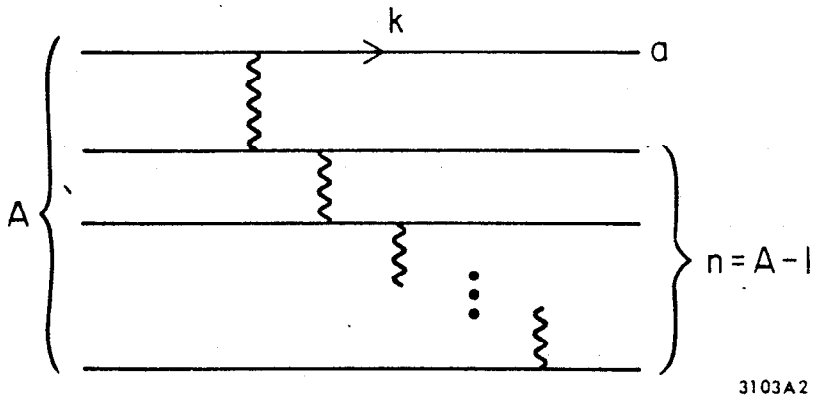

Fig. 2

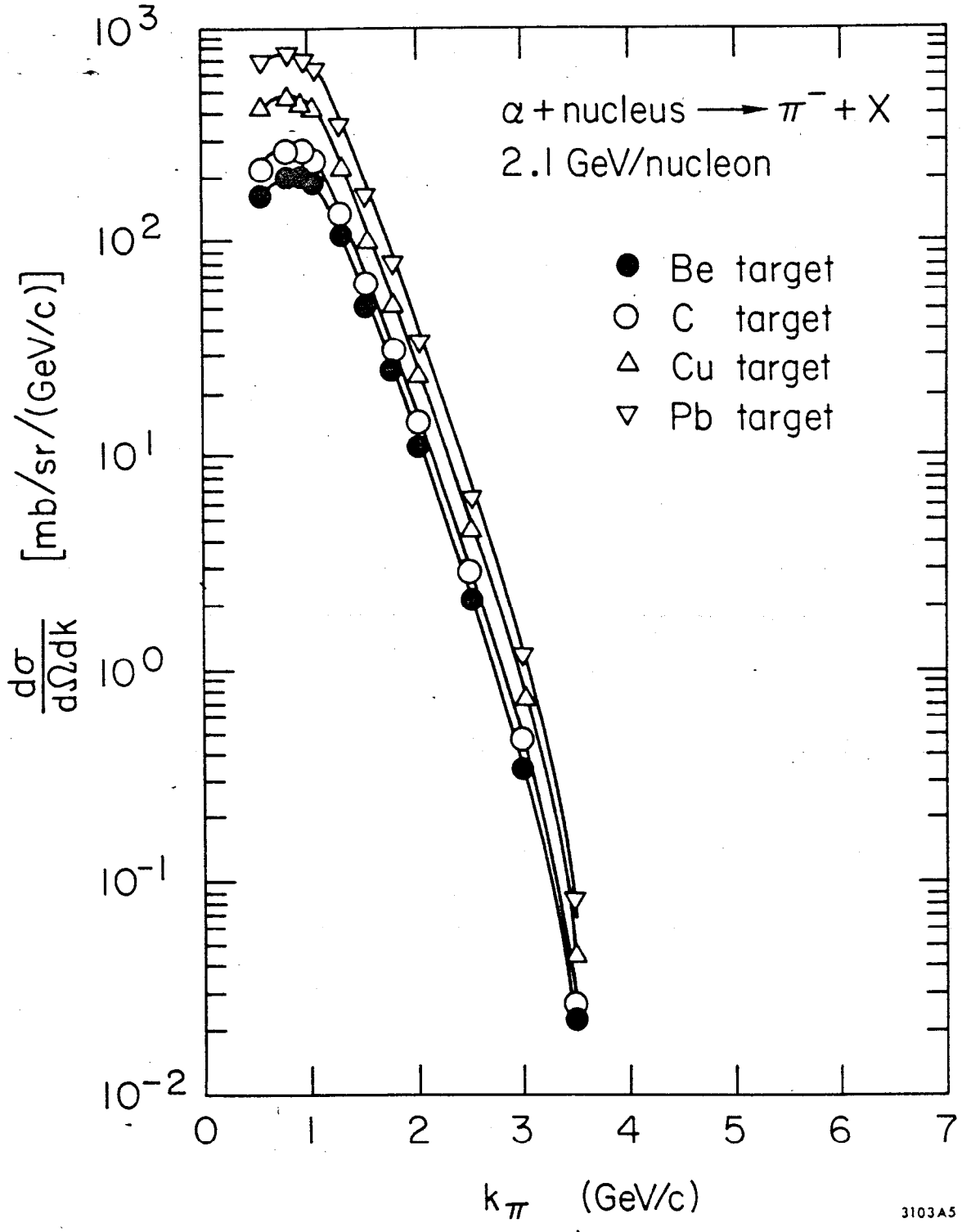
α + nucleus → π⁻ + X
2.1 GeV/nucleon
Be target
C target
Cu target
Pb target
dσ/dΩdk [mb/sr/(GeV/c)]
10³
10²
10¹
10⁰
10⁻¹
10⁻²
0
1
2
3
4
5
6
7
k_π (GeV/c)
3103A5

Fig. 3

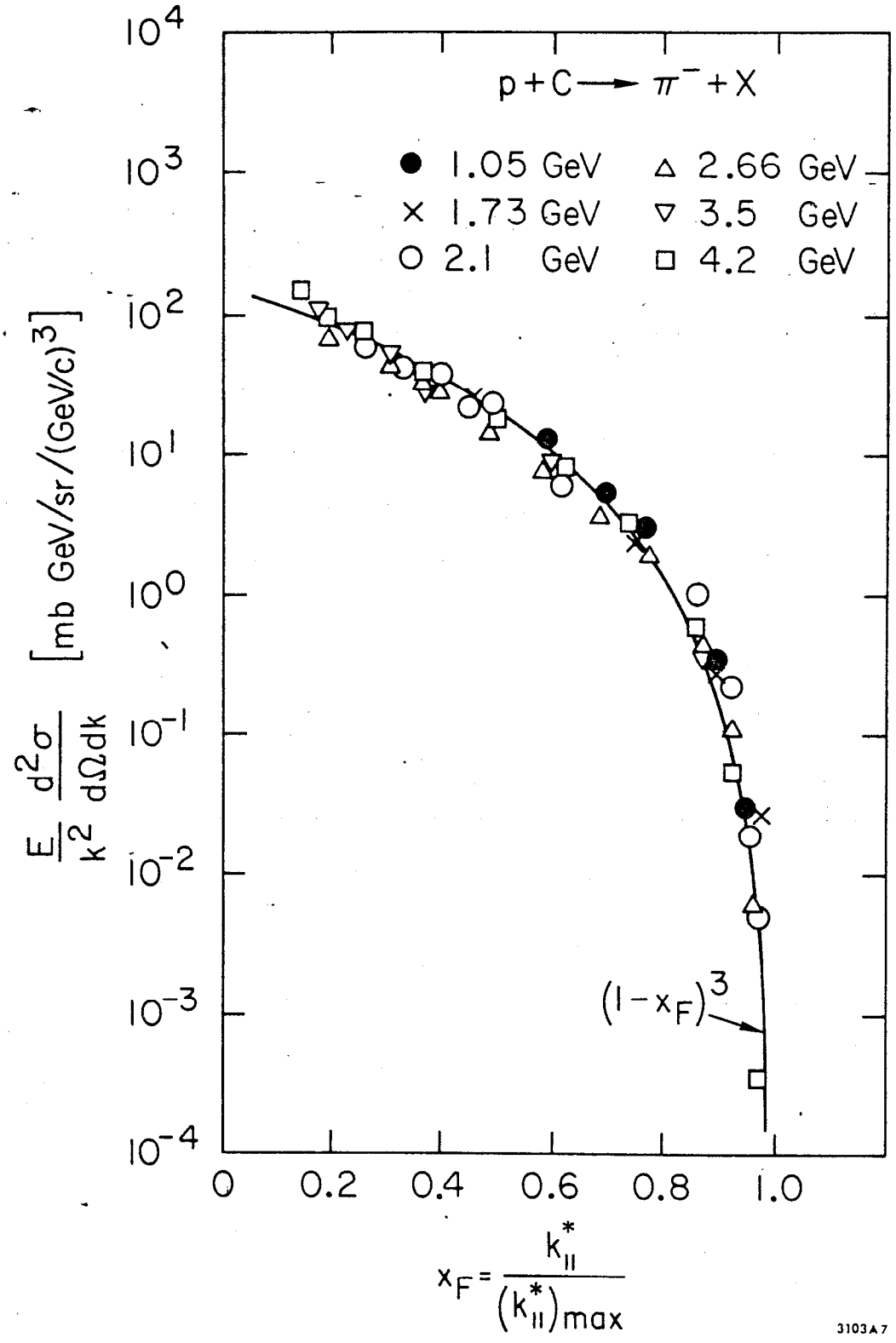
p + C → π⁻ + X
● 1.05 GeV
× 1.73 GeV
○ 2.1 GeV
△ 2.66 GeV
▽ 3.5 GeV
□ 4.2 GeV
$\frac{E}{k^2}\frac{d^2\sigma}{d\Omega dk}$ [mb GeV/sr/(GeV/c)^3]
10^4
10^3
10^2
10^1
10^0
10^{-1}
10^{-2}
10^{-3}
10^{-4}
$(1-x_F)^3$
0
0.2
0.4
0.6
0.8
1.0
$x_F = \frac{k_{||}^*}{(k_{||}^*)_{max}}$
3103A7

Fig. 4

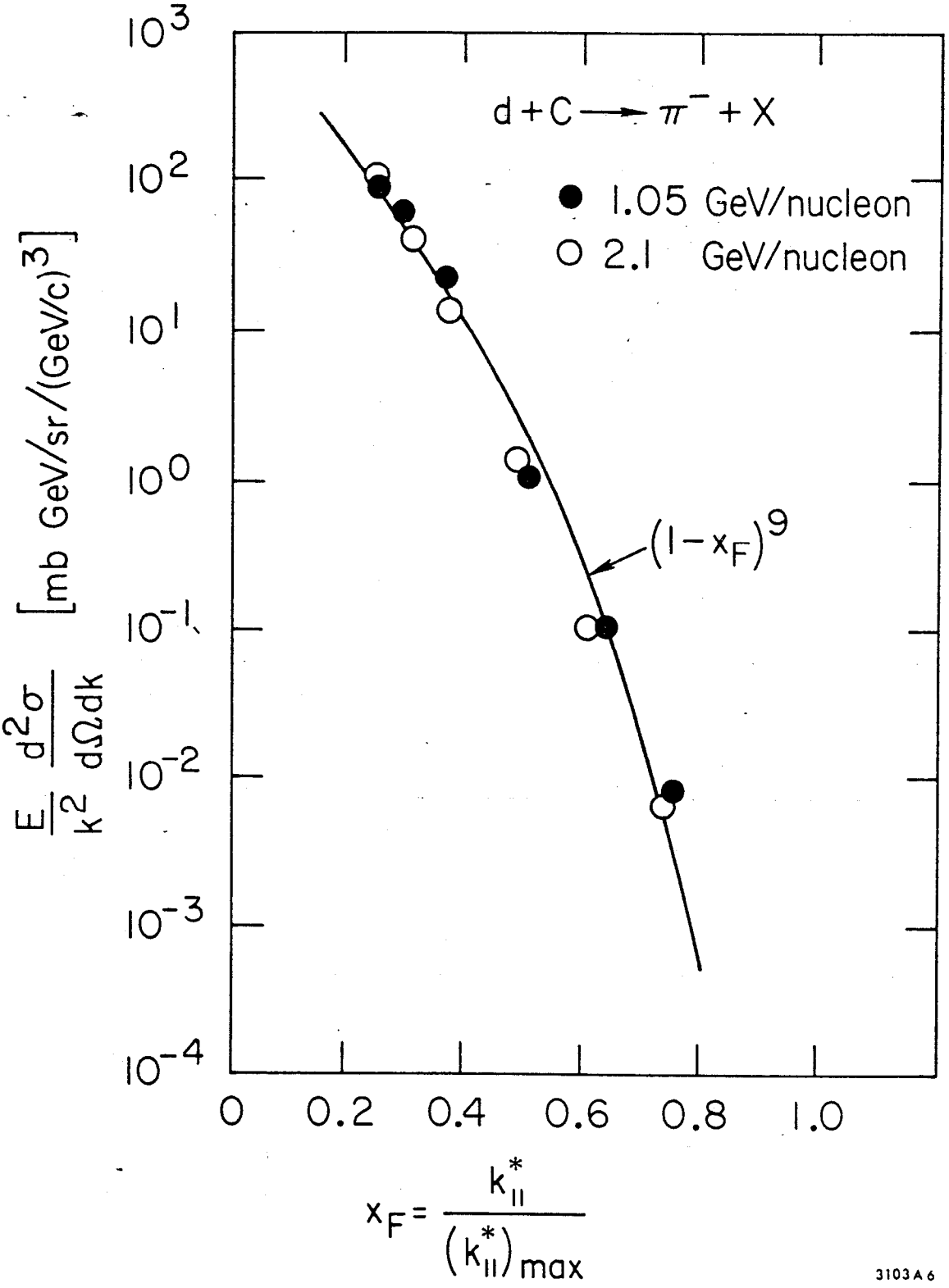
10^3
10^2
10^1
10^0
10^{-1}
10^{-2}
10^{-3}
10^{-4}
$d+C \longrightarrow \pi^- + X$
1.05 GeV/nucleon
2.1 GeV/nucleon
$(1-x_F)^9$
$\frac{E}{k^2}\frac{d^2\sigma}{d\Omega dk}$ [mb GeV/sr/(GeV/c)^3]
0
0.2
0.4
0.6
0.8
1.0
$x_F = \frac{k^*_{II}}{(k^*_{II})_{max}}$
3103A6

Fig. 5

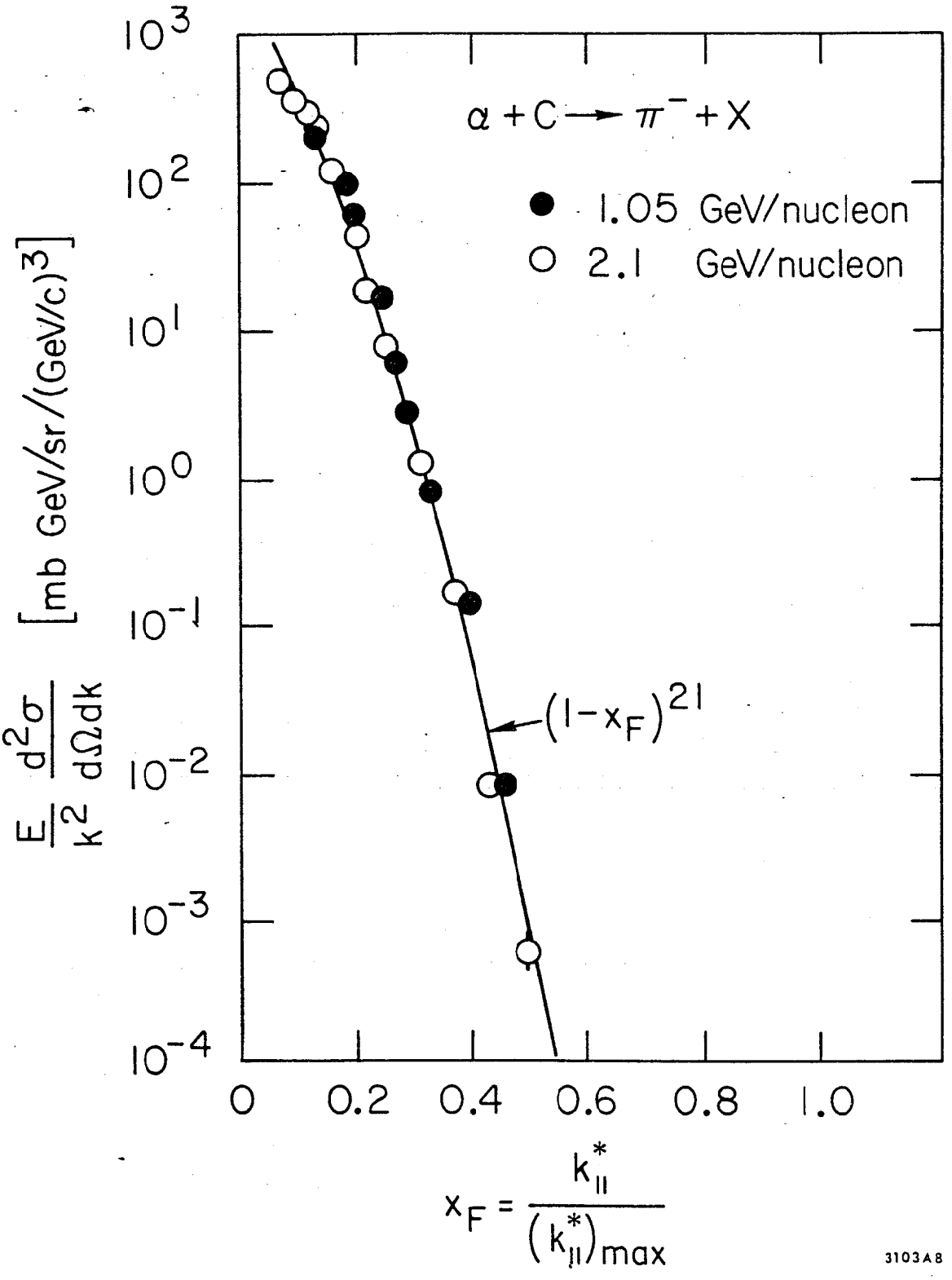
$\alpha + C \rightarrow \pi^- + X$
1.05 GeV/nucleon
2.1 GeV/nucleon
$(1-x_F)^{21}$
$\frac{E}{k^2}\frac{d^2\sigma}{d\Omega dk}$ [mb GeV/sr/(GeV/c)^3]
10^3
10^2
10^1
10^0
10^{-1}
10^{-2}
10^{-3}
10^{-4}
0
0.2
0.4
0.6
0.8
1.0
$x_F = \frac{k^*_{||}}{(k^*_{||})_{max}}$
3103A8

Fig. 6

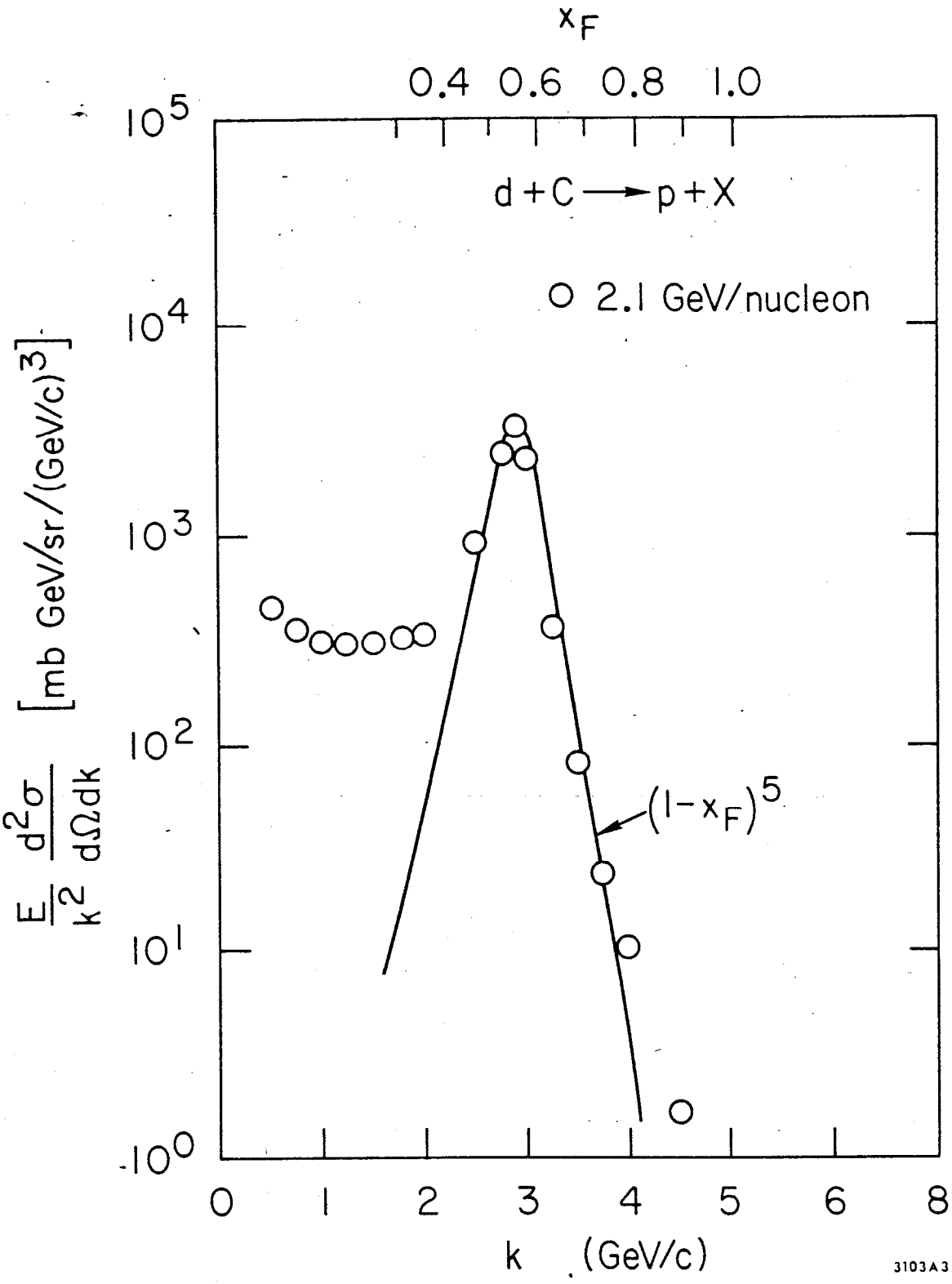
x_F
0.4 0.6 0.8 1.0
10^5
10^4
10^3
10^2
10^1
10^0
d + C → p + X
O 2.1 GeV/nucleon
$\frac{E}{k^2}\frac{d^2\sigma}{d\Omega dk}$ [mb GeV/sr/(GeV/c)^3]
$(1-x_F)^5$
0 1 2 3 4 5 6 8
k (GeV/c)
3103A3

Fig. 7

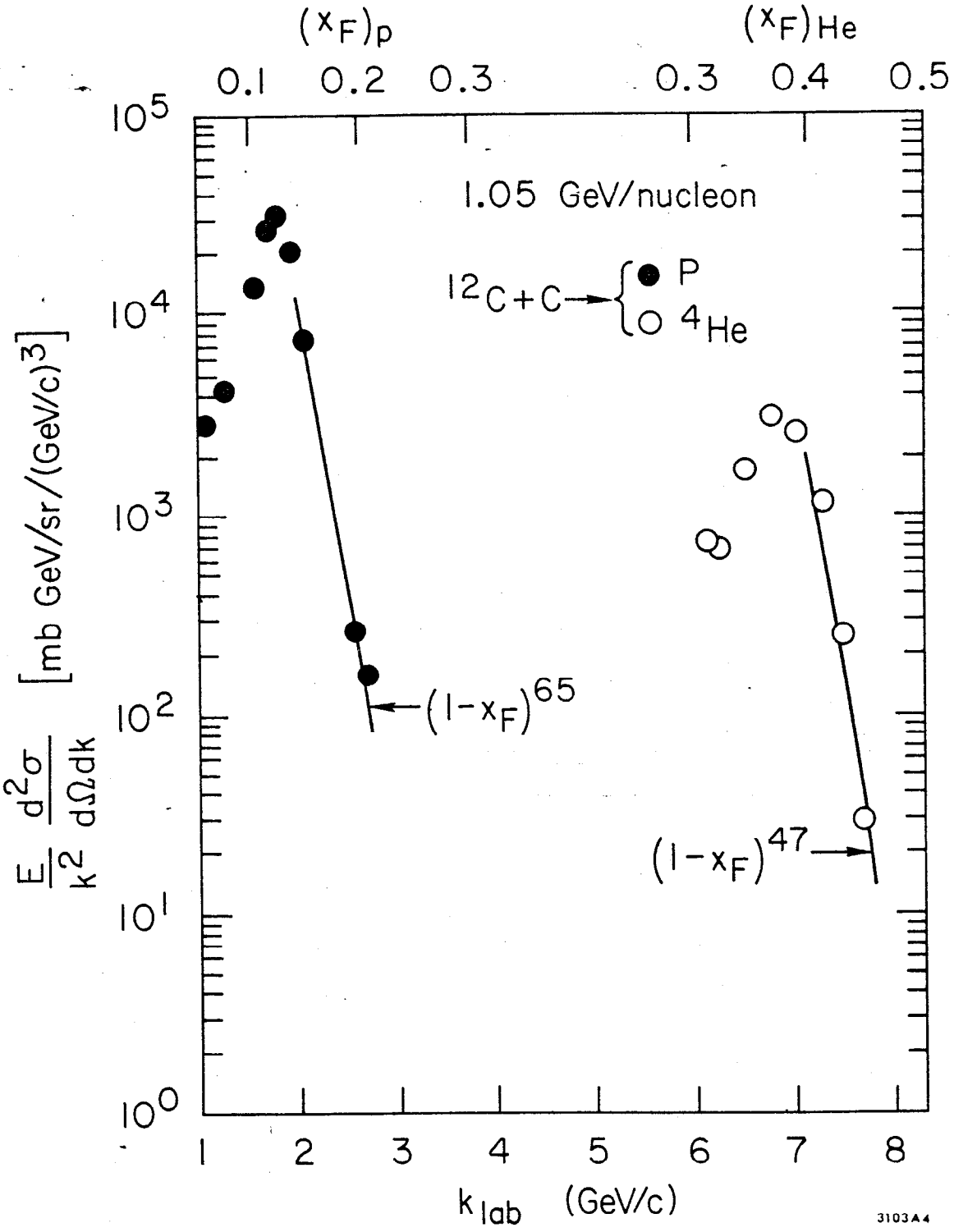
$(x_F)_p$
$(x_F)_{He}$
0.1
0.2
0.3
0.3
0.4
0.5
10^5
10^4
10^3
10^2
10^1
10^0
1.05 GeV/nucleon
$^{12}C+C \rightarrow$ P
^4He
$(1-x_F)^{65}$
$(1-x_F)^{47}$
$\frac{E}{k^2}\frac{d^2\sigma}{d\Omega dk}$ [mb GeV/sr/(GeV/c)^3]
1
2
3
4
5
6
7
8
k_{lab} (GeV/c)
3103A4

Fig. 8